

VLA HI LINE OBSERVATIONS OF THE EXTREMELY METAL-POOR BLUE COMPACT DWARF GALAXY SBS 0335-052

SIMON A. PUSTILNIK

Special Astrophysical Observatory, Russian Academy of Sciences, and Isaac Newton Institute of Chile, SAO
Branch, Nizhniy Arkhyz, 369167, Russia

ELIAS BRINKS

Departamento de Astronomía, Universidad de Guanajuato, Gto 36000 México

TRINH X. THUAN

Astronomy Department, University of Virginia, Charlottesville VA 22903

VALENTIN A. LIPOVETSKY¹

Special Astrophysical Observatory, Russian Academy of Sciences, Nizhniy Arkhyz, 369167, Russia

AND

YURI I. IZOTOV

Main Astronomical Observatory, National Academy of Sciences of Ukraine, 03680, Kyiv, Ukraine

Draft version October 29, 2018

ABSTRACT

We present the results of HI mapping with the NRAO^a VLA of one of the most metal-deficient blue compact dwarf (BCD) galaxies known, SBS 0335-052, with an oxygen abundance of only 1/40 that of the Sun. We study the structure and dynamics of the neutral gas in this chemically young object with a spatial resolution of $20''.5 \times 15''$ ($\sim 5.4 \times 3.9$ kpc at an assumed distance of 54.3 Mpc), a sensitivity at the 2σ detection level of ~ 2.0 K or 7.5×10^{19} cm⁻² and a velocity resolution of 21.2 km s⁻¹. We detected a large HI complex associated with this object with an overall size of about 66 by 22 kpc and elongated in the East-West direction. There are two prominent, slightly resolved peaks visible in the integrated HI map, separated in the East-West direction by 22 kpc (84''). The eastern peak is nearly coincident with the position of the optical galaxy SBS 0335-052. The western peak is about a factor of 1.3 brighter in the HI line and is identified with a faint blue compact dwarf galaxy, SBS 0335-052W, with $m_B = 19.4$, and a metallicity close to the lowest values known for BCDs, about 1/50 that of the Sun. The radial velocities of both systems are similar, suggesting that the two BCDs SBS 0335-052 and SBS 0335-052W constitute a pair of dwarf galaxies embedded in a common HI envelope. Alternatively, the BCDs can be the nuclei of two distinct interacting primordial HI clouds.

The estimated total dynamical mass, assuming the BCDs form a bound system, is larger than $\sim 6 \times 10^9 M_\odot$. This is to be compared to a total gaseous mass $M_{gas} = 2.1 \times 10^9 M_\odot$, and a total stellar mass $M_{star} \leq 10^8 M_\odot$. Hence, the mass of the SBS 0335-052 system is dominated by dark matter. Because of the disturbed HI velocity field and the presence of what might be tidal tails at either end of the system, we favor the hypothesis of tidal triggering of the star formation in this system. It can be due to either the nearby giant galaxy NGC 1376 or the mutual gravitational interaction of the two HI clouds.

^aThe National Radio Astronomy Observatory is operated by Associated Universities, Inc., under contract with the National Science Foundation.

Subject headings: galaxies: compact – galaxies: dwarf – galaxies: evolution – galaxies: individual (SBS 0335-052) – galaxies: ISM – ISM: HI – galaxies: kinematics and dynamics

1. INTRODUCTION

Galaxy formation remains a key issue in observational cosmology. While much progress has been made in finding large populations of galaxies at high ($z > 3$) redshifts (e.g. Steidel et al. 1996; Dey et al. 1998), truly young galaxies in the process of forming, defined as objects which are experiencing their first epoch of star formation, remain elusive. The spectra of those distant galaxies generally indicate the presence of a substantial amount of heavy elements, implying previous star formation and metal enrichment.

We adopt here a different approach for studying truly

young galaxies. Instead of searching for high redshift objects, we look for nearby young dwarf galaxies which are possibly undergoing their first burst of star formation. As pointed out more than a quarter of a century ago by Sargent & Searle (1970) and Searle & Sargent (1972), some low-mass galaxies in the local Universe may approximate galaxies in an early stage of their formation. Later, Thuau & Martin (1981) identified blue compact dwarf (BCD) galaxies as a class of low-luminosity ($M_B \gtrsim -18$) extragalactic systems undergoing a strong burst of star formation (SF) while exhibiting extremely low heavy element abundances.

¹Deceased 1996, September 22.

For many years the best candidate for a truly young galaxy has been I Zw 18 \equiv Mkn 116, with a metallicity Z of about $1/50 Z_{\odot}$ (e.g. Lequeux et al. 1979). Studies of this galaxy in the last decade suggest indeed that it is chemically unevolved. Its extremely low metallicity derived from the HII region-like spectrum has been confirmed by many subsequent studies (see Izotov & Thuan (1998) and references therein). Observations in neutral hydrogen (HI) show that it is a very gas-rich system (Lequeux & Viallefond 1980; Viallefond et al. 1987; van Zee et al. 1998a). Also, its HI gas appears to have an extremely low metallicity (Kunth et al. 1994), although this last point is considered controversial (Pettini & Lipman 1995; van Zee et al. 1998a).

Until the end of the eighties, I Zw 18 remained the only BCD with a heavy element abundance as low as $Z_{\odot}/50$. Despite efforts by many investigators to search for BCDs with equally low or lower metallicities there remained a significant gap in metallicity between I Zw 18 and all other known BCDs. This gap was partially filled when Izotov et al. (1990), using the Russian 6-m telescope, tentatively determined the BCD SBS 0335-052 to have a metallicity lower than that of I Zw 18. However, later Melnick et al. (1992) concluded that $Z = 1/41 Z_{\odot}$ in SBS 0335-052, making it the second most metal-deficient galaxy known in the Universe. This BCD is now considered as one of the best candidates for a galaxy in formation.

A dwarf galaxy experiencing its first burst of star formation should have an extremely low metallicity in its HII regions. Such a galaxy should not show any sign of an older stellar population produced in previous SF episodes. The gas mass would be expected to significantly exceed that in stars. Studies of SBS 0335-052 over the last few years show that it appears to fulfill all those conditions and that it is very probably a truly young galaxy. We briefly summarize its main observational properties :

1. The oxygen abundance in the brightest HII region in the galaxy is found to be $12 + \log(\text{O/H}) = 7.30 \pm 0.01$ (with variations from 7.15 to 7.33 on small scales), only slightly higher than that in I Zw 18 (Melnick et al. 1992; Izotov et al. 1997; Izotov et al. 1999).

2. Blue underlying, extended low-intensity emission is detected in SBS 0335-052 on V , R and I -band images. The blue ($V - I$) and ($R - I$) color distributions suggest that a significant contribution to the emission of the extended low-intensity envelope is due to ionized gas. It is found that the observed equivalent width of $\text{H}\beta$ emission in the extended envelope is 2–3 times weaker than the value expected in the case of pure gaseous emission. This could be explained by the presence of underlying stellar emission from coeval A stars (Izotov et al. 1997; Thuan et al. 1997).

3. From the optical colors of the low surface-brightness component together with evolutionary synthesis models, Papaderos et al. (1998) conclude that the age of the underlying stellar population is less than ~ 100 Myr, with a total mass of $\sim 10^7 M_{\odot}$, comparable with the total mass of young blue stars (Izotov et al. 1997). Near-infrared (NIR) colors after correction for the gas contribution are consistent with a stellar population not older than 4 Myr and the possible contribution to the NIR light from an evolved stellar population in SBS 0335-052 cannot exceed $\sim 15\%$ (Vanzi et al. 2000).

4. No evidence for strong, narrow $\text{Ly}\alpha$ emission is found in a UV spectrum obtained with the *Hubble Space Telescope* (*HST*) (Thuan & Izotov 1997). Instead, a damped $\text{Ly}\alpha$ absorption line is observed which implies an HI column density $N(\text{HI}) = 7 \times 10^{21} \text{ cm}^{-2}$, the largest observed so far for a BCD and comparable to the highest column densities observed in $\text{Ly}\alpha$ clouds in the direction of quasars. The resonant $\text{O I } \lambda 1302$ line is also detected. Assuming that the O I line is unsaturated and that it originates in the neutral gas leads to an oxygen abundance in the neutral gas of $\sim 1/37000$ of the solar value, or about 1/900 of that in the HII regions around the young super-star clusters. However, a more consistent interpretation of the UV absorption lines of O, Si and S is that these lines originate not in the HI but in the HII gas. If this interpretation is correct, then the neutral gas in this system can be pristine and not polluted with heavy elements at all (Thuan & Izotov 1997).

5. Thuan et al. (1995) and Izotov & Thuan (1999) have also argued on the basis of the very small dispersion of the C/O and N/O ratios in extremely metal-deficient BCDs with a metallicity less than $1/20$ solar, that in those galaxies, C and N are made exclusively by massive ($M > 9 M_{\odot}$) stars, because intermediate-mass ($3 M_{\odot} \leq M \leq 9 M_{\odot}$) stars have not had time to evolve and release their nucleosynthesis products. Izotov & Thuan (1999) suggest that BCDs with $Z < Z_{\odot}/20$ are young, with ages less than ~ 100 Myr, the main-sequence lifetime of a $9 M_{\odot}$ star being ~ 40 Myr. Chemical abundances thus also suggest that SBS 0335-052, with $Z = Z_{\odot}/40$, might be a young galaxy.

In view of the unusual properties of this candidate young galaxy we considered it important to measure its neutral gas content and study the HI structure and velocity field. Measurements of the integrated HI flux of this galaxy in the 21-cm line were carried out with the Nançay radio telescope (NRT) in 1993 (Thuan et al. 1999a). From that data the total HI mass was estimated which indicates that this galaxy is gas rich ($M_{\text{HI}} \sim 10^9 M_{\odot}$) with less than a tenth of its baryonic mass in stars. The HI flux appeared to be high enough to allow higher resolution mapping with the VLA. In this paper we present the results of VLA observations of SBS 0335-052 and discuss the properties of its HI density distribution and velocity field.

The paper is organized as follows. In section 2 we describe the observations and data reduction. In section 3 we derive the HI density distribution and velocity field. In section 4 we examine the gas and dynamical mass of the system and in section 5 we focus on various aspects related to the star formation in SBS 0335-052. The paper is summarized in Section 6.

2. OBSERVATIONS AND DATA REDUCTION

The blue compact dwarf galaxy SBS 0335-052 was observed with the VLA in the 21-cm line of neutral hydrogen on December 26, 1994 for an on-source time of 163 min in the C configuration, and on May 13, 1995 for an on-source time of 80 min in the D configuration. The C configuration, with baselines between 160 to 15000 wavelengths (or 0.03 to 3 km) was used to achieve high enough angular resolution in HI to resolve features comparable in size to the optical size of the galaxy ($\sim 15''$). The D configuration, with baselines between 160 to 5000 wavelengths (or

TABLE 1
OBSERVATIONAL PARAMETERS

Parameter	Value	Value
Date	26 Dec 94	13 May 95
VLA configuration	C	
No. of antennae	26	26
Time on source [min]	163	80
Central velocity [km s ⁻¹]	4043	4043
Half-power beam	20'5×15''	61''×45''
Brightness temperature [K] corresponding to 1 mJy beam ⁻¹	2.0	0.22
Total bandwidth [MHz]	3.12	3.12
Total no. channels	31	31
Channel width [km s ⁻¹]	21.2	21.2
Noise in channel maps [mJy beam ⁻¹]	0.5	1.0
Total bandwidth [MHz]	1.56	1.56
Total no. channels	63	63
Channel width [km s ⁻¹]	5.3	5.3
Noise in channel maps [mJy beam ⁻¹]	1.0	2.0

0.03 to 1 km), was used to achieve high surface brightness sensitivity for gas distributed at larger scales (the 2σ noise level corresponds to 7.5×10^{19} cm⁻²) and to search for companion HI clouds, such as those detected near several other BCDs by Taylor et al. (1993, 1995, 1996a), Taylor (1997). Table 1 summarizes the observations.

The observations exploited the 4IF correlator mode. In this mode one IF pair was used to take data over a bandwidth of 1.56 MHz, with 63 channels, giving a channel width of 24.4 kHz (5.3 km s⁻¹), while the second IF pair was used over a 3.12 MHz bandwidth with 31 channels, each having a width of 97.7 kHz (21.2 km s⁻¹). The higher velocity resolution provides detailed information on the galaxy, whereas the lower velocity resolution data cover a larger range in velocity space, at higher S/N ratio.

The data were edited and calibrated with the NRAO AIPS package. The C and D configuration observations were calibrated separately and inspected. Once satisfied with the result, the data were combined and Fourier transformed. In the end, data cubes were obtained measuring 512 × 512 pixels, each pixel measuring 5'' on a side. The resulting synthesized beam was 20'5 × 15''. The noise in the final cube, at a velocity resolution of 21.2 km s⁻¹, is ~ 0.5 mJy/beam in a single channel.

3. HI DISTRIBUTION AND VELOCITY FIELD

In Figures 1 and 2 we show the individual channel maps over the velocity range where significant signal is detected. The size of the synthesized beam is indicated by the ellipse in the lower left hand corner of the first channel map in each of the two figures. Fig. 1 displays the HI emission associated with SBS 0335–052 which is traced in the channels corresponding to a range in velocity from 4000 to 4085 km s⁻¹. Despite the low signal-to-noise in the channel

maps, one can appreciate the rather complex kinematics of the gas. There is an underlying rotation, with the eastern edge of the HI complex receding. A prominent feature in the data cube is a large, almost face-on spiral galaxy, NGC 1376. The channel maps corresponding to the velocities covered by this object are presented in Fig. 2. Its velocity ranges from 4064 to 4234 km s⁻¹. The central radial velocity, 4162 km s⁻¹ (Rix & Zaritzky 1995), is about 120 km s⁻¹ higher than that of our target galaxy.

Adopting a Hubble constant $H_0 = 75$ km s⁻¹ Mpc⁻¹, the redshift distance is 54.3 Mpc (Thuan et al. 1997), so that 1'' corresponds to 263 pc. If NGC 1376 lies at the same distance as SBS 0335–052, their projected distance of about 9.5' then corresponds to 150 kpc.

Fig. 3 is a grey scale presentation of the integrated intensity of the HI in the target field. It is obtained by creating a zeroth moment map of a blanked data cube, i.e., a data cube where all signal below the 2σ level was deleted and in which only those regions are preserved which show emission in at least two successive channels. Both SBS 0335–052 and NGC 1376 are displayed. Notice the elongated structure of the SBS 0335–052 HI cloud with two prominent concentrations separated by about 84'' (or 22 kpc). These “peaks” are marked respectively by “E” and “W” on the map. They are slightly resolved, as indicated by gaussian fitting of the brightness distribution of small regions centered on these peaks, and are situated approximately symmetrically relative to the cloud center. The western peak is about a factor of 1.3 brighter than its eastern counterpart. The HI cloud as a whole is quite inhomogeneous.

Both the E and W HI peaks are embedded in a common, elongated envelope with a strong bend at the eastern edge. The outermost contour in Fig. 3 corresponds to a HI col-

TABLE 2
COORDINATES OF REFERENCE STARS USED
TO TIE THE OPTICAL TO THE VLA
COORDINATE FRAME

Star	$\alpha_{(1950.0)}$	$\delta_{(1950.0)}$
1	03 ^h 34 ^m 59 ^s .71	-05°13'04"0
2	03 ^h 35 ^m 02 ^s .64	-05°12'05"9
3	03 ^h 35 ^m 16 ^s .93	-05°13'19"7
4	03 ^h 35 ^m 19 ^s .23	-05°11'57"7
5	03 ^h 35 ^m 21 ^s .42	-05°10'29"8
6	03 ^h 35 ^m 26 ^s .86	-05°10'50"6

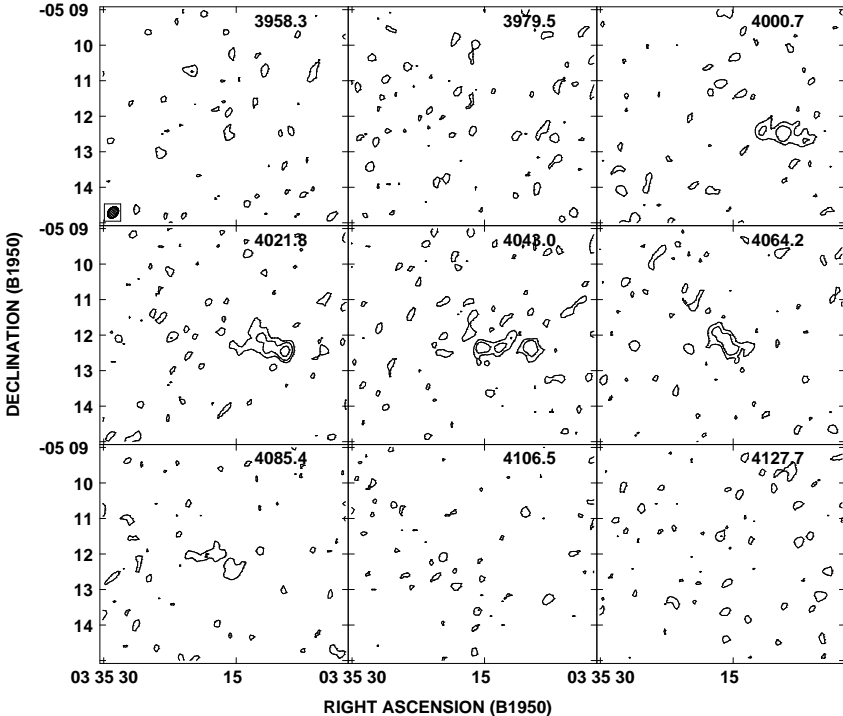


FIG. 1.— Mosaic of channel maps of the low velocity resolution data showing the HI distribution of SBS 0335-052. Contours represent 1 (2 σ), 2, 4 and 6 mJy beam $^{-1}$. The ellipse in the lower left hand corner of the panel on the upper left indicates the beam size.

umn density of 3×10^{20} cm $^{-2}$ and a size of about 31×7 kpc. At the 2σ level above the noise (represented by the lightest grey scale tones in Fig. 3), which corresponds to a HI column density of 1.9×10^{20} cm $^{-2}$, the total extent of the HI emission is $\sim 66 \times 22$ kpc. Some additional weak HI features may be present in the field around SBS 0335-052, including an extended object to the NE. However, these detections are tentative at best and should be confirmed with future higher S/N observations. The structure of the HI feature to the NE of the SBS 0335-052 HI complex at $\delta = -05^\circ 09' 30''$ is quite unusual. No cases similar to this one were found in studies devoted to a search for HI companions near HII galaxies (Taylor et al. 1993, 1995) or low-surface-brightness (LSB) dwarf galaxies (Taylor et al. 1996b).

We should like to emphasize that an HI envelope of this size is rare among BCDs and dwarf irregulars. The typical

size of HI envelopes around BCDs is usually a few kpc (see for example the discussion in Viallefond & Thuan (1983) and in van Zee et al. (1998b)). The only known HI envelope of comparable size is that of HI 1225+01 (Chengalur et al. 1995).

Figure 4 represents the integrated profile of the HI cloud associated with SBS 0335-052. It was calculated by integrating all the flux in the region around SBS 0335-052, as seen in Figure 3. The dashed lines are used to indicate separately the integrated profiles of the eastern and western halves of the HI cloud. Whereas the integrated profile width measured with the VLA is close, within the errors, to that measured with the NRT (Thuan et al. 1999a), the VLA integrated flux of 2.46 ± 0.18 Jy km s $^{-1}$ is about a factor of two higher than that measured with the NRT (1.28 ± 0.22 Jy km s $^{-1}$). This difference points to a significant loss of integrated flux for the NRT due to its narrow

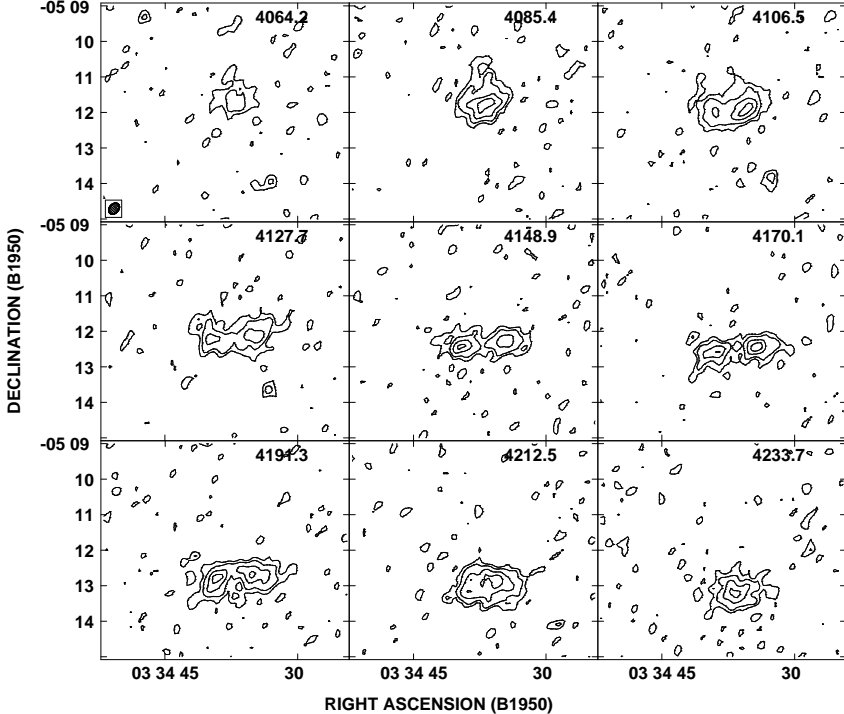


FIG. 2.— Mosaic of channel maps of the low velocity resolution data showing the HI distribution of the bright spiral galaxy NGC 1376. Contours represent 1 (2σ), 2, 4, 6 and 8 mJy beam $^{-1}$. The ellipse in the lower left hand corner of the panel on the upper left indicates the beam size.

horizontal beam (FWHM = 3.5') as compared to the larger extent of up to $\sim 4'$ of the HI cloud in the EW direction. After a first order correction for the NRT beam shape, the NRT/VLA flux ratio becomes 0.78 ± 0.27 , which is consistent within the errors.

Fig. 5 is an overlay of the HI contours on top of an optical B -band image from Papaderos et al. (1998). The optical astrometry was done with the six stars marked by crosses. Their coordinates were obtained from the *Hubble Space Telescope Guide Star Catalog* (Lasker et al. 1990) and are given in Table 2. As shown first by Pustilnik et al. (1997) the two HI peaks are clearly identified with two faint optical galaxies — the eastern one with the object SBS 0335-052 itself, and the western peak with a very compact, faint dwarf galaxy with $m_B = 19.4$. A comparison of the optical and HI peak positions will be given in section 4. No 20 cm continuum emission was detected at the locations of SBS 0335-052, SBS 0335-052W or NGC 1376 at the 4 σ level of 1 mJy. To avoid as much as possible confusion, we will use the same nomenclature for the HI components as for the optical counterparts, referring to the eastern HI component simply as SBS 0335-052 and to the western one as SBS 0335-052W. When referring to the entire HI complex we will employ the term SBS 0335-052 system.

In Fig. 6 we show an enlarged image of the integrated HI flux distribution in the SBS 0335-052 system, the grey scale being a linear representation of the integrated HI flux, with superimposed isovelocities lines with a contour interval of 5 km s^{-1} . The velocity field of the HI gas is quite complex. There is a general gradient across the system from 4085 km s^{-1} at the eastern edge to 4000 km s^{-1} on the western rim. However, there are clear deviations from this general trend near the E and W peaks. This

is perhaps better illustrated in Fig. 7 which is a position-velocity (P-V) diagram made along a line through the two peaks and based on the low velocity resolution data. If the HI complex is treated as a single system, then there is a velocity gradient across, with a maximum velocity difference of $\sim 80 \text{ km s}^{-1}$ between the two sides. If it is considered however as two distinct HI clouds, then the velocity gradients are solid-body in nature, with maximum velocity differences of $\sim 35\text{--}40 \text{ km s}^{-1}$ within each cloud.

[hbtp]

4. RESULTS

As mentioned in the previous section, we derive an integrated HI flux over the entire region around the cloud of $2.46 \text{ Jy km s}^{-1}$. This corresponds to a total HI mass: $M_{\text{HI}} = 1.68 \times 10^9 M_{\odot}$. Since the blue luminosities of the eastern and western galaxies are respectively $7.3 \times 10^8 L_{\odot}$ and $0.82 \times 10^8 L_{\odot}$, the M_{HI}/L_B of the SBS 0335-052 system is of order 2.1.

Accounting for a mass fraction of 0.245 for helium (Izotov & Thuan 1998), the total gas mass in the system is:

$$M_{\text{gas}} = 2.1 \times 10^9 M_{\odot}.$$

With a Salpeter initial mass function, and lower and upper mass limits of 0.8 and $120 M_{\odot}$ respectively and using the models of Schaerer & Vacca (1998), Papaderos et al. (1998) have derived a total stellar mass for the starburst and underlying stellar components of $3.1 \times 10^6 M_{\odot}$. Lowering the lower mass limit to $0.1 M_{\odot}$ would increase the total stellar mass to $\approx 3.7 \times 10^7 M_{\odot}$. From mid-infrared observations, Thuan et al. (1999b) have found that as much three-quarters of the current star formation activity in SBS 0335-052 can be hidden by dust. Correcting for this effect would bring the total stellar mass to $7.3 \times 10^6 M_{\odot}$ and $8.8 \times 10^7 M_{\odot}$ for lower mass cut-offs of 0.8

TABLE 3
SOME OBSERVED AND DERIVED CHARACTERISTICS OF THE SBS 0335–052 SYSTEM

Parameter	0335–052W	0335–052E	References
$\alpha_{(1950.0)}$ (opt) ^a	03 ^h 35 ^m 09 ^s .53	03 ^h 35 ^m 15 ^s .17	4
$\delta_{(1950.0)}$ (opt)	−05°12'25".2	−05°12'27".6	4
B [mag]	19.37	17.00	1
L_B [$10^8 L_B \odot$]	0.82	7.3	1
optical angular size ["] ^b	14×14	23×20	1
optical linear size [kpc]	3.7×3.7	6×5.3	1
V_{opt} [km s ^{−1}]	4069±20	4060±12	2,3
V_{HI} [km s ^{−1}]	4017±5	4057±5	4
$\alpha_{(1950.0)}$ (HI)	03 ^h 35 ^m 09 ^s .50	03 ^h 35 ^m 15 ^s .21	4
$\delta_{(1950.0)}$ (HI)	−05°12'25".5	−05°12'21".5	4
Peak N_{HI} [10^{20} cm ^{−2}]	9.98	7.42	4
Peak HI mass surface density [M_\odot pc ^{−2}]	8.0	6.0	4
M_B^0	−14.3	−16.7	1
HI angular size ["] ^c	128×67	122×83	4
HI linear size [kpc]	33.7×17.6	32.1×21.8	4
M_{HI} [$M_\odot/10^8$]	8.9	8.0	4
M_{HI}/L_B [$M_\odot/L_B \odot$]	10.8	1.1	4
M_{tot}/L_B [$M_\odot/L_B \odot$]	26.8	2.2	4

^aOptical coordinates derived from DSS-2 images.

^bOptical size corresponding to the isophotal level of 27.5 mag arcsec^{−2} in B (Papaderos et al. 1998).

^cMaximum observed extent of the associated HI gas.

^d $L_B \odot$ is the solar blue luminosity corresponding to $M_B \odot=5.48$

REFERENCES.—1. Papaderos et al. (1998). 2. Lipovetsky et al. (1999). 3. Izotov et al. (1997). 4. This paper.

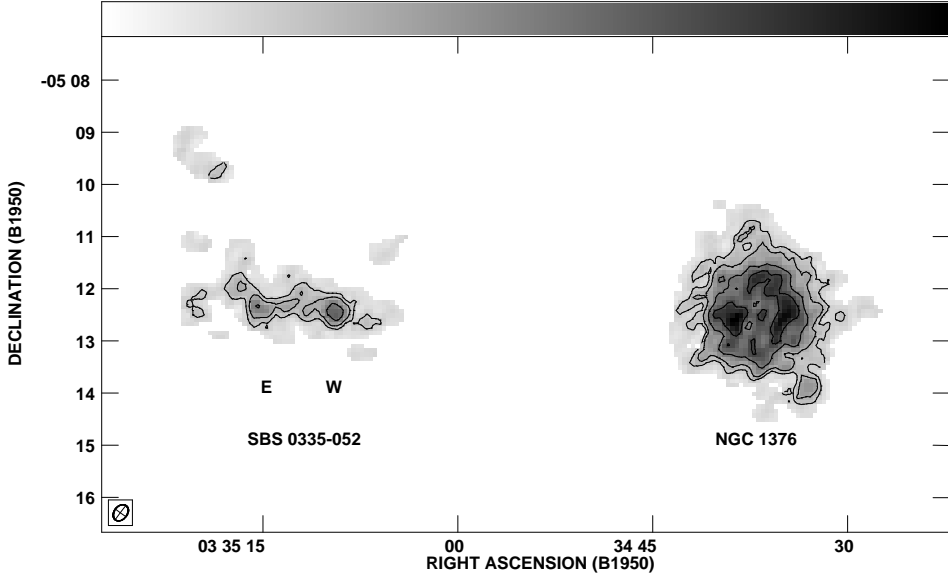


FIG. 3.— Total HI map of SBS 0335-052 and companion galaxy NGC 1376, based on the low velocity resolution data. Contours represent $1.9 (5\sigma)$, 3.8 , 7.6 and $11.4 \times 10^{20} \text{ cm}^{-2}$. The grey scale is a linear representation of HI surface density ranging from 0 (white) to $16 \times 10^{20} \text{ cm}^{-2}$. The ellipse in the lower left hand corner indicates the beam size.

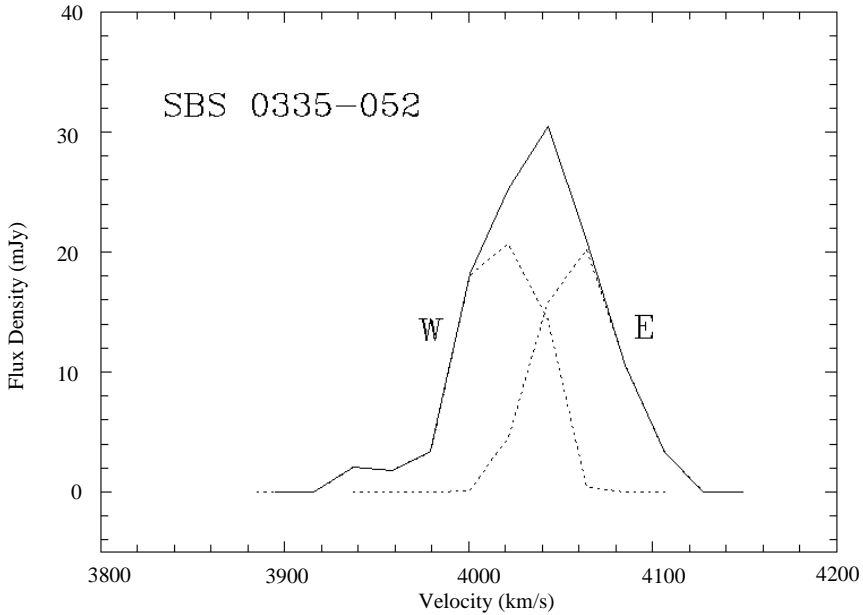


FIG. 4.— Integrated profile of HI flux (in mJy) for the entire HI cloud (solid line) in the system SBS 0335-052, as derived from the channel maps displayed in Fig. 1 for the low velocity resolution data. The total flux, integrated over this profile is $2.46 \text{ Jy km s}^{-1}$. Dashed profiles show integrated profiles for the E and W components separately.

and $0.1 M_{\odot}$ respectively.

Since SBS 0335-052W is about one order of magnitude less luminous and slightly less chemically evolved, its stellar mass is expected to be about 10 times lower than that of the eastern galaxy. Thus the total stellar mass in both dwarf galaxies is at most $10^8 M_{\odot}$, or no more than 5% of the total gas mass.

The two peaks in the distribution of the integrated HI map are partly resolved with the synthesized beam of $20''.5 \times 15''.0$ (or $5.4 \times 3.9 \text{ kpc}$ at the adopted distance of 54.3 Mpc). The position angle of the beam is $\text{PA} = -37^{\circ}$.

We used the AIPS task IMFIT to estimate the properties of both HI peaks. The central brightness of the western peak is 25.8 K km s^{-1} , and its FWHM size after deconvolution with the beam is $(26''.7 \pm 1''.5) \times (15''.6 \pm 1''.5)$ at $\text{PA} = 53^{\circ} \pm 7^{\circ}$. For the eastern peak we get a central brightness of 19.2 K km s^{-1} , and a FWHM size after deconvolution of $(28''.4 \pm 1''.7) \times (12''.7 \pm 4''.9)$ at $\text{PA} = 53^{\circ} \pm 9^{\circ}$. These central brightnesses correspond to a column density of HI:

$$N_{\text{HI}}(\text{west}) = 10.0 \times 10^{20} \text{ cm}^{-2} = 8.0 M_{\odot} \text{ pc}^{-2},$$

$$N_{\text{HI}}(\text{east}) = 7.4 \times 10^{20} \text{ cm}^{-2} = 6.0 M_{\odot} \text{ pc}^{-2}.$$

The faintest regions of the outer HI disk (roughly cor-

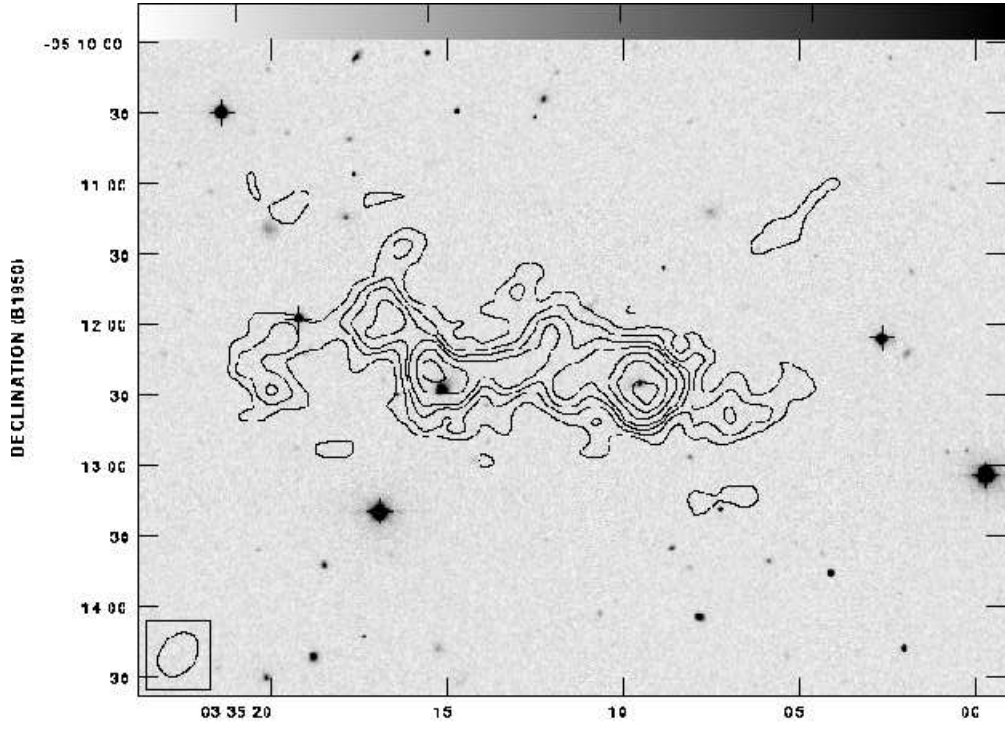


FIG. 5.— Overlay of the HI contours on top of an optical B -band image from Papaderos et al. (1998). The crosses mark the bright stars in the frame which have been used to adjust the overlay. The brightness levels of the B image are presented on a linear scale and in arbitrary units. HI contours represent 0.75 (2σ), 1.8 , 2.7 , 3.6 , 5.4 , 7.2 and 9.0×10^{20} cm $^{-2}$.

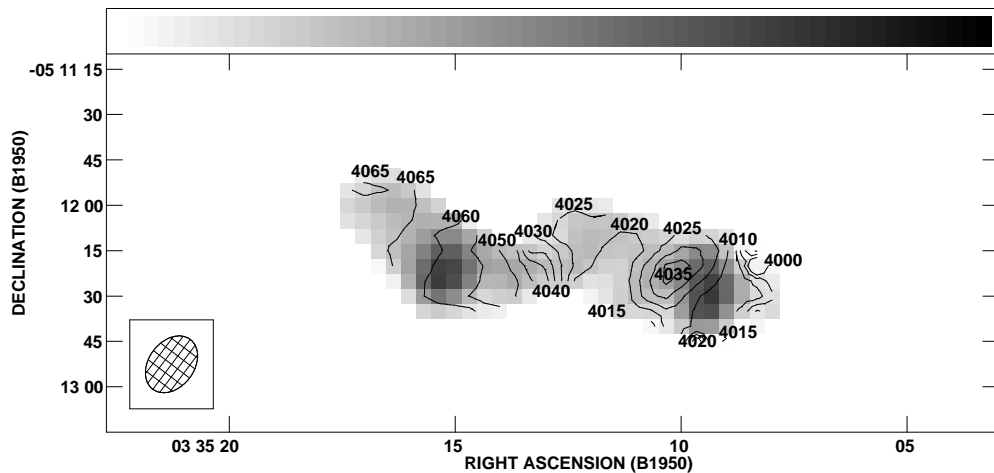


FIG. 6.— Isovelocity lines of HI superimposed on the HI surface brightness map. The grey scale is a linear representation of HI surface density ranging from 0 (white) to $11 \times 10^{20} \text{ cm}^{-2}$.

responding to a 2σ noise level over two consecutive channels) correspond to column densities of $7.5 \times 10^{19} \text{ cm}^{-2}$ or about $0.6 M_{\odot} \text{ pc}^{-2}$. Both HI concentrations are elongated, oriented at the same position angle, roughly SW to NE. Their FWHM angular sizes are very similar and correspond to a linear extent of about $7.1 \times 3.7 \text{ kpc}$. In the SW-NE direction the intrinsic (deconvolved) width of both HI peaks is about a factor of two larger than that of the VLA beam, but in the perpendicular direction it is only $0.7 - 0.8$ of the beam width.

The masses of the eastern and western components, simply dividing the entire cloud in two halves, as was done in Figure 4, leads to gas masses (corrected for He) of:

$$M_{gas}(\text{west}) = 1.11 \times 10^9 M_{\odot},$$

$$M_{gas}(\text{east}) = 0.99 \times 10^9 M_{\odot}.$$

The peak column density, measured for the E-peak, $7.4 \times 10^{20} \text{ cm}^{-2}$ is a factor of 10 lower than the value derived from Ly α absorption based on *HST* observations (Thuan & Izotov 1997). This is also a factor 4 less than the peak brightness of HI for I Zw 18 as derived from VLA

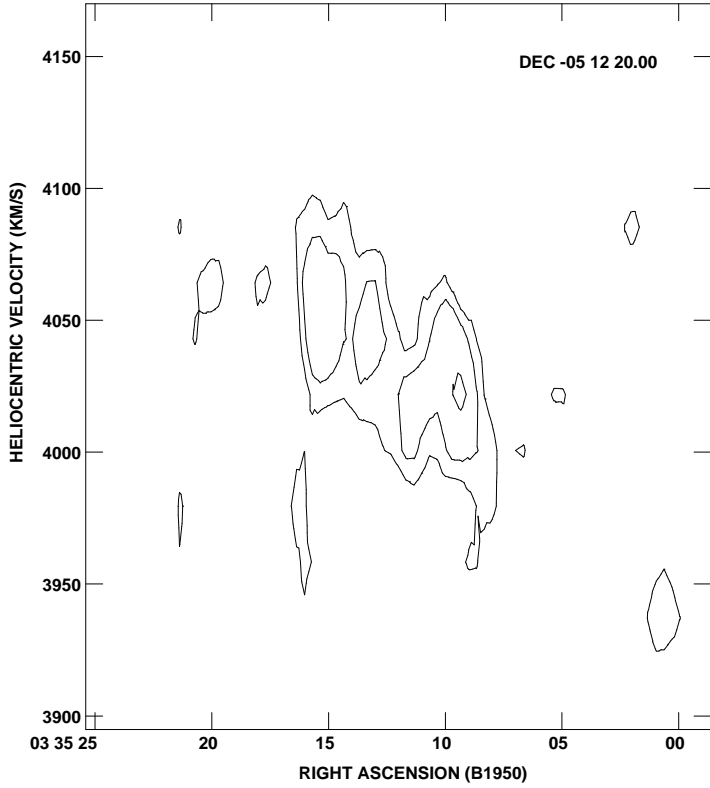


FIG. 7.— Position-velocity slice through the HI emission associated with SBS 0335-052 along an east–west line, cutting through both HI emission peaks referred to as E and W in the text. Contours represent 1.0 (2σ), 2, 4, and 6 mJy beam $^{-1}$. The declination along which the slice was taken is given in the top right corner.

observations by van Zee et al. (1998a) with a synthesized beam $\sim 5''$ (corresponding to a linear resolution of 0.25 kpc). Both facts seem to indicate that despite the fact that some fraction of the brightest parts of the SBS 0335-052 HI complex is resolved by our VLA beam, structure at scales significantly smaller than the beam must exist and that the structure of the neutral gas in the vicinity of the region with high current SF rate is clumpy, explaining the difference in the peak HI column density derived from fitting the damped Ly α line profile (Thuan & Izotov 1997) and that derived here. Probably, an inhomogeneous gas distribution due to HII regions and SNR shells affect the structure of the neutral ISM. Such shell structure is already hinted at by the optical image obtained by Melnick et al. (1992) and confirmed on *HST* images by Thuan et al. (1997).

The coordinates of the HI peaks, determined with the AIPS task IMFIT, as defined by the centers of gaussian components, are presented in Table 3. Their r.m.s. uncertainties are $0\rlap{.}^h18 \times 1\rlap{.}''3$ for the eastern HI peak, and $0\rlap{.}^h11 \times 0\rlap{.}''8$ for the western one.

The optical position of SBS 0335-052W coincides within the errors with the position of the corresponding HI peak. For SBS 0335-052, while there is no shift in right ascension between the optical and HI peaks within the cited errors, there exists a difference in declination $\Delta\delta = +6\rlap{.}''1$. This is more than twice the combined error in declination and seems significant. To check the reality of this offset, we have also compared the optical image with a map made only with the C-configuration data. The displacement is still present. Taken at face value, the shift between the

optical and HI peaks for SBS 0335-052 is about 1.6 kpc, which corresponds to the offsets reported by, e.g., Viallefond & Thuau (1983). Note, however that van Zee et al. (1998a,b), with higher spatial resolution HI maps, find no significant offset between the peaks of the HI and optical intensity distributions in the BCD I Zw 18.

Spectroscopy of the newly discovered galaxy at the position of the western peak with the 6-m (Pustilnik et al. 1997), and with the Multiple Mirror and Keck II telescopes (Lipovetsky et al. 1999) reveals an emission-line spectrum with a radial velocity close to that of the HI cloud. SBS 0335-052W, with an absolute magnitude M_B about -14.3 is, like SBS 0335-052, an extremely metal-deficient object. Its metallicity is 1/50 that of the sun, comparable to that of I Zw 18.

The total dynamical mass is difficult to determine as this depends crucially on one's interpretation of the SBS 0335-052 system. In this paper we will present two strawman hypotheses. The first one is based on the assumption that the system is in fact one cloud with two condensations. The second hypothesis is that we are witnessing the interaction of two systems and that the observed HI shows a tidal bridge between both optical galaxies and tidal tails stretching towards the northeast and to the west.

In the case of one giant cloud, we can estimate the total gravitational mass by equating the centrifugal and gravitational forces at the edges of the disk. We take for the maximum rotational velocity 40 km s^{-1} , and a radius of the disk equal to 16 kpc (Fig. 7). The resulting estimated lower limit for the total dynamical mass is:

$$M_{dyn}(R < 16 \text{ kpc}) = 5.9 \times 10^9 M_{\odot}.$$

In the case of two interacting clouds we estimate, based on the position–velocity diagram (Fig. 7) a full width to zero velocity range of 65 km s^{-1} for SBS 0335–052 and 75 km s^{-1} for SBS 0335–052W. The linear sizes of the HI clouds are at most 12 kpc (this is using the full extent rather than the FWHM along the major axis of each object). We then find:

$$M_{\text{dyn}}(\text{east}) = 1.6 \times 10^9 M_{\odot},$$

$$M_{\text{dyn}}(\text{west}) = 2.2 \times 10^9 M_{\odot},$$

or a total of $M_{\text{dyn}}(\text{east+west}) = 3.8 \times 10^9 M_{\odot}$, 64% of that derived on the basis of the more extreme hypothesis of the objects forming one cloud. It should be noted that these estimates are strict *lower* limits as the inclination is completely unknown and was assumed to be 90° (or edge-on).

We have shown that in both hypotheses, we need to invoke substantial amounts of dark matter in order to reconcile the observed baryonic content with the dynamical masses derived on the basis of the observed kinematics. To obtain yet another (lower) limit to the amount of dark matter which might be hiding within the SBS 0335–052 system, we can take the observed (projected) separation and radial velocity difference and calculate the mass which this implies assuming the two clouds to be in a bound orbit. This works out to be $M_{\text{tot}} = 9 \times 10^9 M_{\odot}$ (see van Moorsel 1987 for details). Therefore, both the individual clouds, as well as the SBS 0335–052 system require substantial amounts of non-visible matter to make up for the inferred masses as based on their dynamics.

5. DISCUSSION

5.1. SBS 0335–052 in relation to other candidate young galaxies

It is interesting to compare this system with other candidate young galaxies. There are three galaxies in the literature with similar characteristics which have been proposed as possible young objects: I Zw 18, ESO 400–G43 and HI 1225+01.

The HI in I Zw 18 has a complex structure with three distinct HI components (Viallefond et al. 1987; van Zee et al. 1998a), two of them associated with star-forming regions: the NW and SE components in the main body of the galaxy and component C to the north (e.g. Dufour et al. 1996). But unlike SBS 0335–052, where the two centers of star formation are well separated spatially, the three star-forming regions in I Zw 18 are connected causally, star formation self-propagating from component C to the SE component (Izotov & Thuan 1998).

In the case of ESO 400–G43 (Bergvall & Jörsäter 1988), the two HI components are well separated by a projected distance of ~ 40 kpc, each component containing an optical counterpart. Only one of the optical galaxies has been studied in detail. It has been described as a possible young galaxy, although its metallicity $Z = Z_{\odot}/8$, is probably too high for it to be forming its first generation of stars (see Izotov & Thuan 1999).

The HI 1225+01 system (Salzer et al. 1991; Chengalur et al. 1995), at a distance of 20 Mpc, presents several similarities to the HI envelope associated with SBS 0335–052. It also has two extended components, separated by a projected distance of 98 kpc, and with an HI tidal bridge linking them. A dwarf HII galaxy 12 kpc in size is located

within the 40 kpc NE HI component, approximately at the position of the HI peak. The total gas mass of the NE HI component of $\sim 3 \times 10^9 M_{\odot}$, is close to that of the HI gas in the SBS 0335–052 system. The dynamical mass is a factor of 3 larger than the gas mass. Due to a smaller inclination angle ($i \sim 30^\circ$) and better spatial and velocity resolution the authors are able to distinguish bar-like and spiral structure in the NE HI component.

The very low metallicity, $Z \sim 1/20 Z_{\odot}$, in the HII region associated with the current SF burst and the very low mass fraction in the form of stars suggest that the HI 1225+01 system probably is in the process of forming its first generation of stars. One of the arguments by Salzer et al. (1991), who claim that the current SF burst in this HII galaxy is possibly not the first one, is that there is a significant abundance of nitrogen, which the authors assume to be produced by intermediate-mass stars. However, as mentioned earlier, the finding of a constant N/O ratio with a very small dispersion in the most metal-poor BCDs, those with $Z < Z_{\odot}/20$ (Thuan et al. 1995; Izotov & Thuan 1999) strongly suggests primary production of nitrogen by massive stars in galaxies as metal-deficient as SBS 0335–052, and thus there is no need for a second burst of star formation in the optical counterpart of HI 1225+01 to account for the nitrogen abundance. The second HI component has no detectable optical emission, but shows a velocity field corresponding to that of an inclined rotating disk. Thus, Chengalur et al. (1995) suggest that the most probable interpretation for this system is a SF burst in a primordial HI cloud (the NE component) due to the tidal action of another massive HI cloud.

The HI properties of the SBS 0335–052 system also show some similarities with those of II Zw 40 (Brinks & Klein 1988; van Zee et al. 1998b). The metallicity of this BCD is $\sim Z_{\odot}/6$, considerably higher than those of the above-mentioned systems, and suggesting that this galaxy is more evolved than SBS 0335–052 and not necessarily its analog. Nevertheless it is instructive to briefly compare the two objects to discuss their different evolutionary states. The II Zw 40 system is most likely a merger, showing two HI tidal tails of ~ 6.5 and 15 kpc in size. The extent of the HI gas and the HI masses of the tails are reminiscent of the situation in SBS 0335–052. However, the optical morphologies of SBS 0335–052 and II Zw 40 differ. Whereas II Zw 40 resembles an advanced merger with optical tidal tails (van Zee et al. 1998b), SBS 0335–052 exhibits two regular-looking still widely separated dwarf galaxies which are perhaps in an earlier stage of what could evolve into a merger. Over time, SBS 0335–052 might very well develop into a system resembling II Zw 40.

5.2. Possible star formation triggers

One of the unsolved problems ever since the discovery of the first BCDs (Sargent & Searle 1970) concerns the triggering mechanism for the star formation. And perhaps even more baffling, why has star formation not occurred earlier in the lifetime of these objects.

In all likelihood, tidal triggering is probably responsible for the current star formation in the SBS 0335–052 system. We shall again consider two hypotheses: 1) the case where SBS 0335–052 is one huge HI cloud containing two star-forming centers; and 2) the BCDs are the nuclei of two distinct interacting HI clouds.

In the case of a single self-gravitating HI cloud, the tidal triggering is probably due to the companion massive galaxy NGC 1376 whose HI map is seen in Figure 8. The resolution of the map is too low to say much about the HI morphology. However we can note that the HI gas is, as usual, more extended than the optical disk, and that there is a conspicuous lack of HI in the nuclear region of the galaxy. A lower limit to the distance between the galaxy and the SBS 0335–052 system is their observed projected distance of 150 kpc. NGC 1376 is an Scd galaxy with $m_{pg} = 12.8$, $M_B = -21.0$, an optical diameter $D = 2'0$ and an inclination of 21° . Its HI profile is characterized by a full width at 20% of peak intensity of 179 km s^{-1} and a heliocentric radial velocity $V_{\text{HI}} = 4162 \text{ km s}^{-1}$. It is a member of a medium density group listed as LGG 103 (Garcia 1993) and composed of at least 14 galaxies. NGC 1376 is situated on its south–western outskirts. The closest known group member is at a projected distance of about 0.7 Mpc. Rix & Zaritsky (1995) note that NGC 1376 has 3 spiral arms, and Elmegreen & Elmegreen (1987), in their classification of spiral galaxies, assign this galaxy to class 2, which means that its arms are “fragmented spiral pieces with no regular pattern”. This suggests that the spiral has recently experienced a tidal disturbance.

The VLA HI data does point to a small galaxy, companion to NGC 1376, that may be at the origin of that tidal disturbance. Fig. 8 shows a small irregular HI blob SW of the main body of NGC 1376 at $\alpha = 03^{\text{h}}34^{\text{m}}32.9^{\text{s}}$ and $\delta = -05^{\circ}13'51''$. Its detection is weak, but fairly reliable as it can be seen in at least two neighboring channel maps, at a heliocentric velocity of $4117 \pm 5 \text{ km s}^{-1}$. Its integrated flux density is $0.17 \text{ Jy km s}^{-1}$, which corresponds to an HI mass of $1.2 \times 10^8 M_{\odot}$ at the distance of 54.3 Mpc. This blob is kinematically detached from the regular velocity field of the galaxy and can be identified optically on the Deep Sky Survey (DSS) with what appears to be a faint elongated dwarf companion, not listed in NED and with a diameter of $\sim 23''$ (i.e. a linear size of $\sim 6 \text{ kpc}$) at a projected distance of 27.5 kpc from NGC 1376. The HI profile of the dwarf galaxy is two channels wide so that its velocity width is $\sim 42 \text{ km s}^{-1}$. This gives a lower limit (the inclination being unknown) of $\sim 2.5 \times 10^8 M_{\odot}$ for its dynamical mass.

The total dynamical mass of NGC 1376, as estimated from the width of the HI profile (inclination corrected to $V_{\text{rot}} = 250 \text{ km s}^{-1}$) and the radius of the HI distribution, is about $5 \times 10^{11} M_{\odot}$. Taking into account the results by Zaritsky & White (1994) and Zaritsky et al. (1997) on distant dwarf satellites of spiral galaxies and masses of their dark matter halos, the total gravitational mass of NGC 1376, exerting a tidal force on SBS 0335–052, can be up to twice that value, or $10^{12} M_{\odot}$. A detailed understanding of the triggering mechanism of a SF burst due to tidal forcing such as due to NGC 1376 is still lacking. It will require a more careful study and modelling which is beyond the scope of this paper. However, it is clear from some simple estimates, that this massive spiral galaxy is close enough to the HI complex to induce in it a gravitational instability via mechanisms such as those suggested by Icke (1985), Noguchi (1988) and Olson & Kwan (1990a,b). The mechanism proposed by Noguchi (1988) generates a central bar, which in turn causes gas to sink

towards the center of the disk and induce its collapse. No observational evidence is seen, neither for a central bar-like structure in the HI cloud of SBS 0335–052, nor for a central density concentration. The mechanism by Olson & Kwan (1990a,b) works via a large tidal increase of the inelastic collision rate of individual gas clouds, and their merging and collapse. It is basically a stochastic process.

The most probable mechanism is that proposed by Icke (1985) involving tidal acceleration to supersonic velocities of gas layers in the external parts of an HI disk, with subsequent dissipation of the kinetic energy and loss of dynamical stability of the gas disk. It takes only a moderate tidal force, and acts from larger distances in comparison with the two other mechanisms. Adopting a radius $R = 16 \text{ kpc}$ for the HI disk and a circular velocity V of 40 km s^{-1} at R , a dynamical mass within R of $6 \times 10^9 M_{\odot}$ for the SBS 0335–052 system, a total dynamical mass of $10^{12} M_{\odot}$ for NGC 1376, and a sound speed of the HI gas of 10 km s^{-1} , we find that for pericenter distances smaller than $\sim 412 \text{ kpc}$, the gas in SBS 0335–052 can be accelerated to supersonic velocities. This distance is significantly larger than the present projected distance of 150 kpc so that sufficiently strong tidal forces of NGC 1376 on the HI complex are expected. Such a tidal triggering mechanism may explain the fact that the two star-forming centers began nearly simultaneously, and are aligned along the line joining the centers of the two objects, symmetrically on either side of the center of the SBS 0335–052 system, just as the tidal forces of the moon on the earth causes high ocean tides on diametrically opposite locations on earth.

Alternatively, we may consider that we do not have a single huge HI complex, but two distinct smaller HI components interacting tidally with each other and triggering star formation at the location of the two HI peaks. In this case, the tidal force F_1 exerted by each cloud is proportional to M (cloud) / d_1^3 where d_1 is the projected separation between the two BCDs. On the other hand, the tidal force F_2 exerted by NGC 1376 is proportional to M (NGC 1376) / d_2^3 where d_2 is the projected separation between the galaxy and the SBS 0335–052 system. Adopting M (cloud) = $2 \times 10^9 M_{\odot}$, M (NGC 1376) = $10^{12} M_{\odot}$, $d_1 = 22 \text{ kpc}$ and $d_2 = 150 \text{ kpc}$, we find $F_1 / F_2 = 0.6$, i.e the tidal forces in the two cases are comparable and we cannot say for sure which of the two scenarios discussed above prevails. In the case of two distinct HI components, we find that the Icke (1985) mechanism will apply for pericenter distances less than $\sim 27 \text{ kpc}$.

Clearly, detailed hydrodynamical calculations of the tidal interaction between two HI clouds and between a massive galaxy like NGC 1376 and a primordial gas cloud similar to that associated with SBS 0335–052, are needed to understand better the triggering of star formation in these systems.

5.3. Star formation threshold

Star formation in disk galaxies is thought to occur above a critical threshold of the gas surface density above which clouds will become gravitationally unstable against collapse (Toomre 1964; Kennicutt 1989). This critical density is proportional to the velocity dispersion of the gas disk and the epicyclic frequency, which is twice the circular frequency for regions with solid body rotation. The validity of the Kennicutt (1989) HI column density thresh-

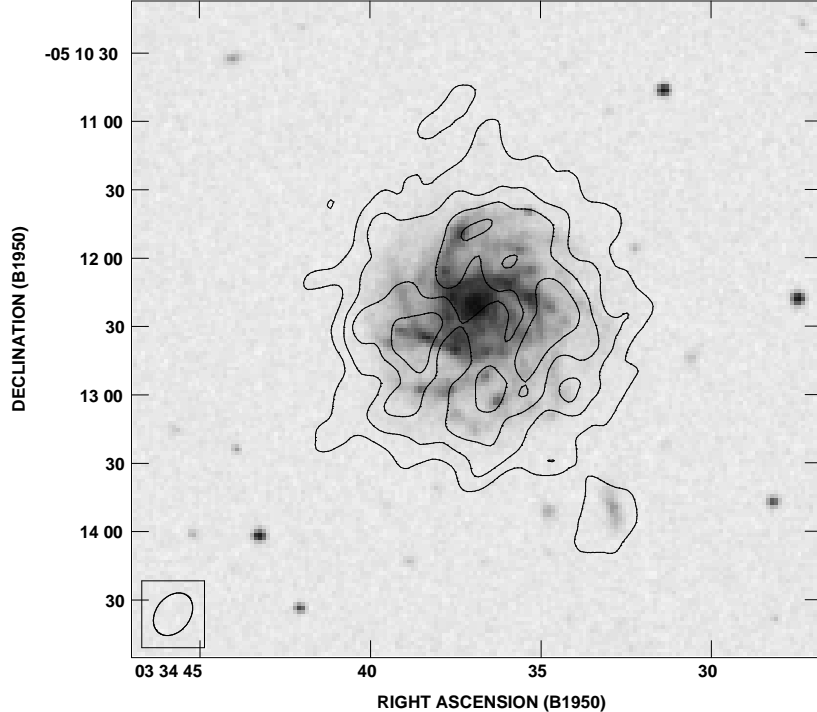


FIG. 8.— Overlay of the HI contours on top of a DSS image of NGC 1376. Contour levels are at $3.8, 7.6, 11.4$ and $15.2 \times 10^{20} \text{ cm}^{-2}$. There is a small HI blob SW of NGC 1376 which coincides with a low-surface-brightness dwarf galaxy not listed in NED.

old for onset of star formation has been checked for BCDs (e.g., Taylor et al. 1994) as well as for LSB galaxies (van der Hulst et al. 1993). Alternatively, as first mentioned by Skillman (1987), star formation in dwarf irregulars occurs when the column densities reach values of order $5 \times 10^{20} \text{ cm}^{-2}$, with this threshold increasing with decreasing metallicity (Franco & Cox 1986).

The observed peak column densities in the SBS 0335-052 system coinciding with the optical counterparts are near the upper end of the range of those reported for HII galaxies by Taylor et al. (1993, 1995) — $(0.8 - 11) \times 10^{20} \text{ cm}^{-2}$ — when compared to data on objects mapped with comparable linear resolution, of order 5 kpc. These values are also in the same range observed for LSB galaxies, — $(1.0 - 10.5) \times 10^{20} \text{ cm}^{-2}$ — objects in which no significant star formation takes place, and observed by van der Hulst et al. (1993) with a similar linear resolution.

Given our modest spatial resolution, all we can do is make an order of magnitude estimate of the expected threshold value and compare that to the observed (beam-smeared) ones. To obtain an estimate we assume that both peaks fall within the solid body part of the rotation curve, at a rotational velocity of about 20 km s^{-1} and a radial distance of 6 kpc. With a typical gas velocity dispersion σ_v of 6 km s^{-1} , we obtain for the critical surface density at the radius of the current SF burst a value equal to only $1.3 M_\odot \text{ pc}^{-2}$ (equation 6 of Kennicutt 1989 with $\alpha = 2/3$), in comparison with measured values of $8.0 M_\odot \text{ pc}^{-2}$ and $6.0 M_\odot \text{ pc}^{-2}$. With a viewing angle of the HI disk of less than 77° , the gravitational instability condition would be satisfied. This appears to be the case since in the simple model of a circular flattened HI disk, the observed axial ratio would correspond to a viewing angle of 70° .

5.4. The role of a dark matter halo

It has been shown (e.g. de Blok et al. 1996) that LSB galaxies are dominated by dark matter over the entire area where HI and stellar emission is detected. This dark matter dominance is one of the main factors which allows an LSB galaxy to be stable against various perturbations (see e.g., the study of the relative fragility of LSB and high-surface-brightness disks by Mihos et al. 1997). If in the SBS 0335-052 system we indeed observe the formation of a first generation of stars in a low density primordial gas cloud, then its dark matter halo should have played an especially important role for stabilizing the gas against various local and global instabilities and preventing it from gravitationally collapsing and forming stars. Presumably, a strong tidal perturbation due either to a close passage of a massive galaxy or to the interaction with another HI cloud can overcome the stabilizing influence of the dark matter halo and trigger a starburst.

6. CONCLUSIONS

From the observational data presented here, and the properties derived for the HI gas and based on the discussion above we arrive at the following conclusions:

1. The optical dwarf galaxy SBS 0335-052 is associated with a huge HI cloud with overall size of $66 \times 22 \text{ kpc}$, elongated in the EW direction. The cloud has a total HI mass of $1.68 \times 10^9 M_\odot$.
2. This HI cloud contains two prominent HI peaks, located nearly symmetrically to the East and West, and separated by about 22 kpc. They measure $7 \times 4 \text{ kpc}$ and contain $0.79 \times 10^9 M_\odot$ and $0.89 \times 10^9 M_\odot$, respectively, of HI.

3. The two HI density peaks are identified with two optical emission-line dwarf galaxies, the eastern one with SBS 0335-052 itself, and the western one with a new, one order of magnitude less luminous dwarf named SBS 0335-052W. This latter galaxy shows very similar properties, including an extremely low metallicity of the HII region gas, consistent with the amount produced during a first SF burst. Radial velocities of these galaxies, as measured from the emission lines of their HII regions are very close to those of the HI gas at the positions of their respective peaks.
4. The velocity field of the HI cloud is rather disturbed, with presumably tidal tails protruding from both edges of the cloud. This suggests that what we are seeing is an interaction, possibly with the nearby galaxy NGC 1376. This large spiral galaxy, the dominant member of the galaxy group LGG 103, with a projected radial velocity of 120 km s^{-1} larger than that of SBS 0335-052, is located at a projected distance of 150 kpc. Consideration of the relevant parameters of the SBS 0335-052 system and NGC 1376 does not contradict the hypothesis that the formation of the two young dwarfs from the huge low-surface density HI cloud was triggered by a tidal interaction with NGC 1376.
5. Alternatively, we are dealing with two almost equal mass HI clouds, each measuring $\sim 7 \times 4 \text{ kpc}$, each containing an optical counterpart, and showing solid-body rotation with an amplitude of $\sim 35\text{-}40 \text{ km s}^{-1}$. In this case, the triggering of the star formation in the two HI clouds is probably due to their mutual tidal interaction.
6. Each component seems to require the presence of dark matter, and the system as a whole is dominated by a dark matter halo. The total dynamical mass of the system is estimated to be between $3.8 \times 10^9 M_\odot$ and $9 \times 10^9 M_\odot$, or ~ 1.9 to 4.5 times larger than the total mass of gas and stars.
7. If the viewing angle of the HI disk is less than 77° , the gas surface densities for both HI peaks are larger than the critical value determined from the parameters of the rotation curve at those radii and are consistent with the onset of gravitational instability and subsequent star formation.

Acknowledgements. We thank the partial financial support of NATO collaborative research grant 921285 (SAP, TXT), INTAS grant No. 94-2285 (SAP, YII), NSF grant AST-9616863 (TXT, YII), Russian grant RFBR 97-02-16755 (SAP) and CONACyT grant No. 0460P-E (EB). SAP is grateful to the NRAO staff at Socorro for hospitality and support with the VLA data reduction, and to Oleg Verkhodanov and Pat Murphy for help with installing AIPS at the Special Astrophysical Observatory. The *B* optical image of the SBS 0335-052 system was kindly provided by Polychronis Papaderos. The anonymous referee made useful suggestions which helped to improve the presentation of the paper. We have made use of the NASA/IPAC Extragalactic Database (NED) which is operated by the Jet Propulsion Laboratory, California Institute of Technology, under contract with the National Aeronautics and Space Administration. We have also used the Digitized Sky Survey which was produced at the Space Telescope Science Institute under US Government grant NAG W-2166.

REFERENCES

- Bergvall, N., & Jörsäter, S. 1988, *Nature*, 331, 589
 Brinks, E., & Klein, U. 1988, *MNRAS*, 231, 63
 Chengalur, J. N., Giovanelli, R., & Haynes, M. P. 1995, *AJ*, 109, 2415
 de Blok, W. J. G., McGaugh, S. S., & van der Hulst, J. M. 1996, *MNRAS*, 283, 18
 Dey, A., Spinrad, H., Stern, D., Graham, J. R., & Chaffee, F. H. 1998, *ApJ*, 498, L93
 Dufour, R. J., Garnett, D. R., Skillman, E. D., & Shields, G. A. 1996, in *ASP Conf. Ser.* 98, *From Stars to Galaxies*, eds. C. Leitherer, U. Fritze - von Alvensleben, & J. Huchra (San Francisco: ASP), p. 358
 Elmegreen, D., & Elmegreen, B. 1987, *ApJ*, 314, 3
 Franco, J., & Cox, D. P. 1986, *PASP*, 98, 1076
 Garcia, A. M. 1993, *A&AS*, 100, 47
 Icke, V. 1985, *A&A*, 144, 115
 Izotov, Y. I., Chaffee, F. H., Foltz, C. B., Green, R. B., Guseva, N. G., & Thuan, T. X. 1999, *ApJ*, 527, 757
 Izotov, Y. I., Lipovetsky, V. A., Chaffee, F. H., Foltz, C. B., Guseva, N. G., & Kniazev A. Y. 1997, *ApJ*, 476, 698
 Izotov, Y. I., Lipovetsky, V. A., Guseva, N. G., Kniazev, A. Y., & Stepanian, J. A. 1990, *Nature*, 343, 238
 Izotov, Y. I., & Thuan, T. X. 1998, *ApJ*, 497, 227
 —. 1999, *ApJ*, 511, 639
 Kennicutt, R. C. 1989, *ApJ*, 344, 685
 Kunth, D., Lequeux, J., Sargent, W. L. W., & Viallefond, F. 1994, *A&A*, 282, 709
 Lasker, B. M., Sturch, C. R., McLean, B. J., Russell, J. L., Jenkner, H., & Shara, M. M. 1990, *AJ*, 99, 2019
 Lequeux, J., Peimbert, M., Rayo, J. F., Serrano, A., & Torres-Peimbert, S. 1979, *A&A*, 80, 155
 Lequeux, J., & Viallefond, F. 1980, *A&A*, 91, 269
 Lipovetsky, V. A., Chaffee, F. H., Izotov, Y. I., Foltz, C. B., Kniazev, A. Y., & Hopp, U. 1999, *ApJ*, 519, 177
 Melnick, J., Heydari-Malayeri, M., & Leisy, P. 1992, *A&A*, 253, 16
 Mihos, J. C., McGaugh, S. S., & de Blok, W. J. G. 1997, *ApJ*, 477, L79
 Noguchi, M. 1988, *A&A*, 203, 259
 Olson, K. M., & Kwan, J. 1990a, *ApJ*, 349, 480
 —. 1990b, *ApJ*, 361, 426
 Papaderos, P., Izotov, Y. I., Fricke, K. J., Guseva, N. G., & Thuan, T. X. 1998, *A&A*, 338, 43
 Pettini, M., & Lipman, K. 1995, *A&A*, 297, L63
 Pustilnik, S. A., Lipovetsky, V. A., Izotov, Y. I., Brinks, E., Thuan, T. X., Kniazev, A. Y., Neizvestny, S. I., & Uglyumov, A. V. 1997, *Astronomy Lett.*, 23, 308
 Rix, W., & Zaritsky, D. 1995, *ApJ*, 447, 82
 Salzer, J. J., Di Serego Alighieri, S., Matteucci, F., Giovanelli, R., & Haynes, M. 1991, *AJ*, 101, 1258
 Sargent, W. L. W., & Searle, L. 1970, *ApJ*, 162, L155
 Schaerer, D., & Vacca, W. D. 1998, *ApJ*, 497, 618
 Searle, L., & Sargent, W. L. W. 1972, *ApJ*, 173, 25
 Skillman, E. D. 1987, in *Star Formation in Galaxies*, ed. C. J. Lonsdale Persson (NASA Conf. Pub. CP-2466), 263
 Steidel, C., Giavalisco, M., Pettini, M., Dickinson, M., & Adelberger, K. 1996, *ApJ*, 462, L17
 Taylor, C. L. 1997, *ApJ*, 480, 524
 Taylor, C. L., Brinks, E., Grashuis, R. M., & Skillman, E. D. 1995, *ApJS*, 99, 427
 —. 1996a, *ApJS*, 102, 189
 Taylor, C. L., Brinks, E., Pogge, R. W., & Skillman, E. D. 1994, *AJ*, 107, 971
 Taylor, C. L., Brinks, E., & Skillman, E. D. 1993, *AJ*, 105, 128
 Taylor, C. L., Thomas, D. L., Brinks, E., & Skillman, E. D. 1996b, *ApJS*, 107, 143
 Thuan, T. X., & Izotov, Y. I. 1997, *ApJ*, 489, 623
 Thuan, T. X., Izotov, Y. I., & Lipovetsky, V. A. 1995, *ApJ*, 445, 108
 —. 1997, *ApJ*, 477, 661
 Thuan, T. X., Lipovetsky, V. A., Martin, J.-M., & Pustilnik, S. A. 1999a, *A&AS*, 139, 1

- Thuan, T. X., & Martin, G. M. 1981, *ApJ*, 247, 823
 Thuan, T. X., Sauvage, M., & Madden, S. 1999b, *ApJ*, 516, 783
 Toomre, A. 1964, *ApJ*, 139, 1217
 van der Hulst, J. M., Skillman, E. D., Smith, T. R., Bothun, G. D.,
 McGaugh, S. S., & de Blok, W. J. G. 1993, *AJ*, 106, 548
 van Moorsel, G. A. 1987, *A&A*, 176, 13
 van Zee, L., Skillman, E. D., & Salzer, J. J. 1998b, *AJ*, 116, 1186
 van Zee, L., Westpfahl, D., Haynes, M., & Salzer, J. J. 1998a, *AJ*,
 115, 1000
 Vanzi, L., Hunt, L. K., Thuan, T. X., & Izotov, Y. I. 2000, *A&A*, in
 press
 Viallefond, F., Lequeux, J., & Comte, G. 1987, in *Starburst and*
 Galaxy Evolution, eds. T. X. Thuan, T. Montmerle & J. T. T.
 Van, Édition Frontières, 139
 Viallefond, F., & Thuan, T. X. 1983, *ApJ*, 269, 444
 Zaritsky, D., Smith, R., Frenk, C., & White, S. D. M. 1997, *ApJ*,
 478, 39
 Zaritsky, D., & White, S. 1994, *ApJ*, 435, 599